22

Computer Simulation of Involute Tooth Generation

Cuneyt Fetvaci
Istanbul University, Mechanical Engineering Department, Turkey

1. Introduction

Gearing is an essential component of many machines. From aerospace to high-speed automation, from missiles to submarines, few machines can operate without gears. Involute gears are the most popular power transmission devices for parallel axes owing to their simple geometry, easy manufacturing, and constant gear ratio even when the centre distance has been changed. Spur gears are the most popular form and the most efficient type of gearing for the cost when transmitting power and uniform rotary motion from one parallel shaft to another.

In mass production of gears, generating-type cutters are used. According to the type of relative motion between cutter and gear blank, generating cutters are classified as: rack cutters, hob cutters and gear shapers. Generation cutting is based on the fact that two involute gears of the same module and pitch mesh together - the gear blank and the cutter. This method makes to use one cutter for machining gears of the same module with a varying number of teeth. Rack-type cutters (rack or hob) can only generate external gears. Both external and internal gears can be generated by a pinion-type cutter. Figure 1 displays generating-type cutters.

For cylindrical gears in applications with uniform load-rotation conditions, an optimized and separate design of traction and thrust flank is desirable. This can be achieved by using different pressure angles for traction and thrust flank, which results in asymmetric tooth geometries. The load-carrying capacity of the gear mechanism can be improved without disturbing the material quality by using asymmetric profiles (Muni et al., 2007).

The computer simulation of gear cutting enables us to investigate the influence of design parameters on the generated profile before manufacturing. Undercutting and zero topland can be detected in design phase. Also the physical behaviour of the gear under operating conditions can be simulated and investigated. Therefore possible faults due to the inaccurate design can be detected for preventing time and material lost. An accurate geometrical representation of gear tooth surfaces is the fundamental starting point for developing a reliable computerized gear design which includes tooth contact analysis and stress analysis. Therefore, a good knowledge of the gear geometry is required.

Based on analytical mechanics of gears, parametric equations describing involute profile and root fillet profile of the gear teeth have been derived for hobbed and shaped gears (Buckingham, 1949; Colbourne, 1987; Litvin, 1994; Salamoun & Suchy, 1973). Litvin applied the vector analysis, differential geometry, matrix transformation and meshing equation to develop mathematical models for describing tooth profiles and their geometric properties (Litvin, 1994). Tsay proposed the mathematical model of the involute helical gears generated by rack-type cutters (Tsay, 1988). Chang and Tsay proposed a complete mathematical model of noncircular gears, including the fillets, bottom lands and working surfaces of tooth profiles manufactured by involute-shaped shaper cutters (Chang & Tsay, 1998). Figliolini and Angeles studied the generation of noncircular gears manufactured by the sharp-edge involute-shaped shaper cutters (Figliolini & Angeles, 2003). Chen and Tsay developed the mathematical models of helical gear sets with small numbers of teeth manufactured by modified rack- and pinion-type cutters (Chen & Tsay, 2005). Yang proposed the mathematical models of asymmetric helical external gears generated by rack-type cutters and internal gears generated by shaper cutters (Yang, 2005, 2007). Fetvaci has adopted Chang and Tsay's model to pinion-type shapers with asymmetric involute teeth for generating internal and external gears (Fetvaci, 2010a, 2011).

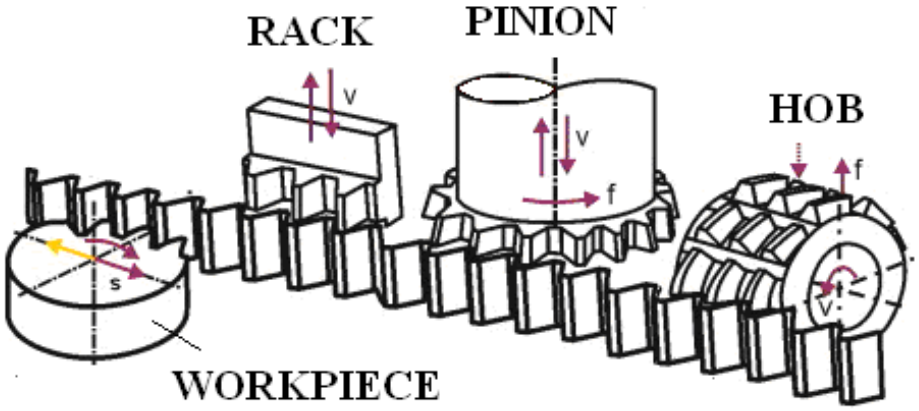

Fig. 1. Meshing of generating cutters and generated gear (Bouzakis et al., 2008)

The shape of the fillet has a direct effect on the motion/force transmission and eventual maximum bending stresses developed at the root of the gear tooth. The fillet curve of the gear belongs to the trochoid family and it is conjugate to the tip of the generating cutter. The equations for the root fillet of the spur and helical gears have been proposed by many authors in literature (Buckingham, 1949; Colbourne, 1987; Litvin, 1994; Salamoun & Suchy, 1973). Also the machining parameters of generating cutter have been given for rack-type and pinion-type cutters with two round edges or single round edge (Lin et al., 2007). During the generating process of spur gear tooth, the center of the rounded corner at the tip traces out a trochoid. Then the rounded tip envelopes another curve called as secondary trochoid, defining the root fillet. Su and Houser studied the application of trochoids to find exact fillet shapes generated by rack-type cutters (Su & Houser, 2000). Fetvaci and Imrak have adapted the equations of trochoids given by Su and Houser to Yang's mathematical model for spur

gears with asymmetric involute teeth (Fetvaci & Imrak, 2008). Besides, simulated motion path of the rack cutter has been illustrated. Fetvaci has studied trochoidal paths of the pinion-type cutter during the generation of internal and external spur gears with asymmetric involute teeth (Fetvaci, 2010a, 2011).

The relative positions of the cutter during gear teeth generating process can be used for determining chip geometry for further analysis on tool wear and tool life. Tang et al. presented a computer simulation method of spur gear generating process with the sharp edge rack- and pinion-type cutters using Visual Lisp as programming language and AutoCAD as graphical display tools (Tang et al., 2008). Fetvaci presented computer simulation methods for generating asymmetric involute spur gears with rounded edge generating cutters (Fetvaci, 2010a, 2010b, 2011).

In this study, accurate mathematical models of the generating-type cutters for spur gear production are given, and trochoidal paths that determine the shape of generated tooth root fillet are investigated. Indirect gear design depending on the pre-selected set of cutting tool parameters is considered. Based on the mathematical models, computer codes have also been developed to compute the coordinates of the gear tooth profile generated by different types of cutters like cutter with sharp tip, partially round and full round tip for symmetric and asymmetric involute spur gears. Computer graphs are obtained to visualise the effect of tool parameters on generated gears before manufacturing.

The content of this chapter is organized as follows: In Section 2, the matematical models of generating cutter surfaces are studied according to Litvin's vector approach. The mathematical models: the locus of the rack- and pinion-type cutter surfaces, the equation of meshing and the generated gear tooth surfaces are given in Section 3. Trochoidal paths of the cutter tips are investigated in Section 4. As a result, Section 5 deals with computer simulation of the generating process for the verification and the validation of the matematical models. Simulated motion path of the cutter during generation process is also illustrated. The varieties of the cutter tip geometry are investigated. Finally, a conclusive summary of this study is given in Section 6.

2. Generating tooth surfaces

2.1 Rack cutter surfaces

For simplicity, the generation of spur gears with shaper cutters can be simplified into a two-dimensional problem. Due to the asymmetry of the rack cutter, left and right sides of the cutter are considered seperately. Figure 2. presents the design of the normal section of a rack cutter Σ_n, where regions $\overline{ac}$ and $\overline{bd}$ are the left- and right-side top lands, regions $\overline{ce}$ and $\overline{df}$ are the left- and right-side fillets and, regions $\overline{eg}$ and $\overline{fh}$ are the left- and right-side working regions.

The regions $\overline{ac}$ and $\overline{bd}$ are used to generate the bottomland of asymmetric spur gear and l_a and l_b represent design parameters of normal section of the rack cutter. In order to generate complete profile of the rack cutter surface a tooth of rack cutter will be repeated for $c_y = 0,1,2,..$. Equations of regions $\overline{ac}$ and $\overline{bd}$ of the rack cutter normal section can be represented in the coordinate system $S_n(X_n, Y_n, Z_n)$ by the following equations (Yang, 2005).

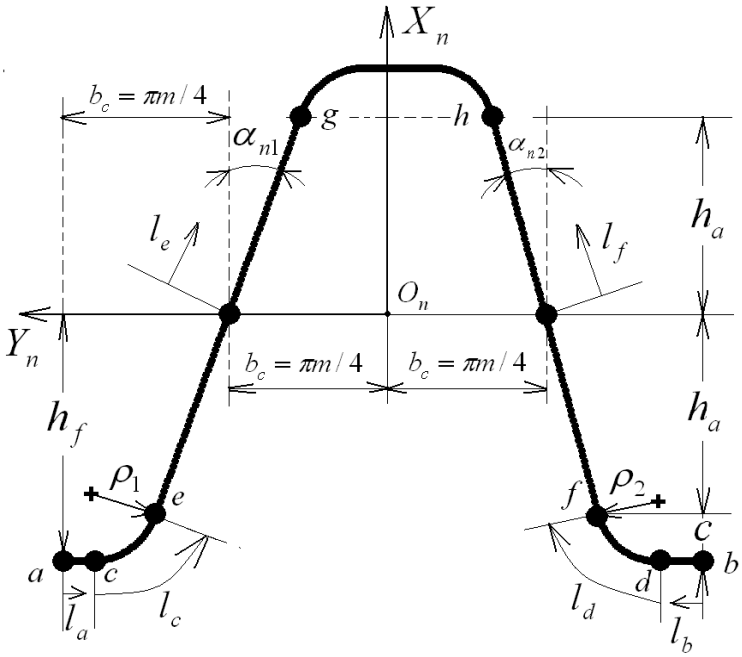

Fig. 2. Normal section of the rack cutter with asymmetric teeth (Fetvaci, 2011; Yang, 2005)

$$\mathbf{R}_n^{ac} = \begin{Bmatrix} x_n^{ac} \\ y_n^{ac} \end{Bmatrix} = \begin{Bmatrix} -h_a + \rho_1 \sin\alpha_{n1} - \rho_1 \\ (\frac{\pi m_n}{2} - l_a + c_y \pi m_n) \end{Bmatrix} \tag{1}$$

and

$$\mathbf{R}_n^{bd} = \begin{Bmatrix} x_n^{bd} \\ y_n^{bd} \end{Bmatrix} = \begin{Bmatrix} -h_a + \rho_2 \sin\alpha_{n2} - \rho_2 \\ (-\frac{\pi m_n}{2} + l_b + c_y \pi m_n) \end{Bmatrix} \tag{2}$$

where design parameters l_a and l_b are limited by $0 \le l_a \le b_c - h_a \tan\alpha_{n1} - \rho_1 \cos\alpha_{n1}$ and $0 \le l_b \le b_c - h_a \tan\alpha_{n2} - \rho_2 \cos\alpha_{n2}$ on the left- and right-side of the cutter respectively.

As depicted in Fig.1., regions $\overline{ce}$ and $\overline{df}$ on the normal section of the rack cutter generate different sides of the fillet surface of the gears. l_c and l_d are the design parameters of the rack cutter surface which determine the location of points on the fillets. The position vectors of regions $\overline{ce}$ and $\overline{df}$ are represented in the coordinate system S_n as follows (Yang, 2005) :

$$\mathbf{R}_n^{ce} = \begin{Bmatrix} x_n^{ce} \\ y_n^{ce} \end{Bmatrix} = \begin{Bmatrix} -h_a + \rho_1 \sin\alpha_{n1} - \rho_1 \cos l_c \\ (b_c + h_a \tan\alpha_{n1} + \rho_1 \cos\alpha_{n1} - \rho_1 \sin l_c + c_y \pi m_n) \end{Bmatrix} \tag{3}$$

and

$$\mathbf{R}_n^{df} = \begin{Bmatrix} x_n^{df} \\ y_n^{df} \end{Bmatrix} = \begin{Bmatrix} -h_a + \rho_2 \sin\alpha_{n2} - \rho_2 \cos l_d \\ (-b_c - h_a \tan\alpha_{n2} - \rho_2 \cos\alpha_{n2} + \rho_2 \sin l_d + c_y \pi m_n) \end{Bmatrix} \tag{4}$$

where design parameters l_c and l_d are limited by $0 \le l_c \le 90° - \alpha_{n1}$ and $0 \le l_d \le 90° - \alpha_{n2}$ respectively.

As shown in Fig. 1., two straight edges $\overline{eg}$ and $\overline{fh}$ of the rack cutter are used to generate the left- and right-side tooth surface of the asymmetric helical gear, respectively. The symbol m_n represents the normal module. The position vector of regions $\overline{eg}$ and $\overline{fh}$ are represented in the coordinate system S_n as follows (Yang, 2005):

$$\mathbf{R}_n^{eg} = \begin{Bmatrix} x_n^{eg} \\ y_n^{eg} \end{Bmatrix} = \begin{Bmatrix} l_e \cos\alpha_{n1} \\ (b_c - l_e \sin\alpha_{n1} + c_y \pi m_n) \end{Bmatrix} \tag{5}$$

and

$$\mathbf{R}_n^{fh} = \begin{Bmatrix} x_n^{fh} \\ y_n^{fh} \end{Bmatrix} = \begin{Bmatrix} l_f \cos\alpha_{n2} \\ (-b_c + l_f \sin\alpha_{n2} + c_y \pi m_n) \end{Bmatrix} \tag{6}$$

where l_e and l_f are the design parameters of the rack cutter surface which determine the location of points on the working surface. l_e and l_f are limited by $-h_a / \cos\alpha_{n1} \le l_e \le h_a / \cos\alpha_{n1}$ and $-h_a / \cos\alpha_{n2} \le l_f \le h_a / \cos\alpha_{n2}$ for the left- and right-side of the rack cutter respectively. The surface unit normals of the regions $\overline{ac}$ to $\overline{fh}$ of the rack cutter surfaces are represented by (Litvin, 1994),

$$\mathbf{n}_n^i = \frac{\dfrac{\partial \mathbf{R}_n^i}{\partial l_j} \times \mathbf{k}_n}{\left| \dfrac{\partial \mathbf{R}_n^i}{\partial l_j} \times \mathbf{k}_n \right|} \quad \begin{matrix} (i = ac \sim fh) \\ (j = a \sim f) \end{matrix} \tag{7}$$

where $\mathbf{k}_n$ is the unit vector of the Z_n-axis.

2.2 Pinion-type shaper cutter surfaces

Pinion-type shaper cutters are designed consists of six generating regions as depicted in Fig.3. Regions 1 and 6 of the involute-shaped curves generate the working regions of involute spur gears, regions 2 and 5 of the circular arcs with centers at *E* and *G* generate the fillet surfaces, and regions 3 and 4 of the shaper cutter surfaces generate the bottom lands (Chang & Tsay, 1998). Based on (Figliolini & Angeles, 2003), nongenerating surfaces of the cutter are also shown for visual purposes only.

In Fig. 3, coordinates systems $S_s(X_s, Y_s)$ and $S_c(X_c, Y_c)$ represent the reference and the shaper cutter coordinate systems, respectively. According to the relationship between coordinate systems S_s and S_c, the position vector of region i can be transformed from

coordinate systems S_s to S_c by applying the following homogeneous coordinate transformation (Litvin, 1994):

$$R_c^i = \begin{Bmatrix} x_c^i \\ y_c^i \end{Bmatrix} = \begin{bmatrix} \sin\psi & -\cos\psi \\ \cos\psi & \sin\psi \end{bmatrix} \begin{Bmatrix} x_s^i \\ y_s^i \end{Bmatrix} \tag{8}$$

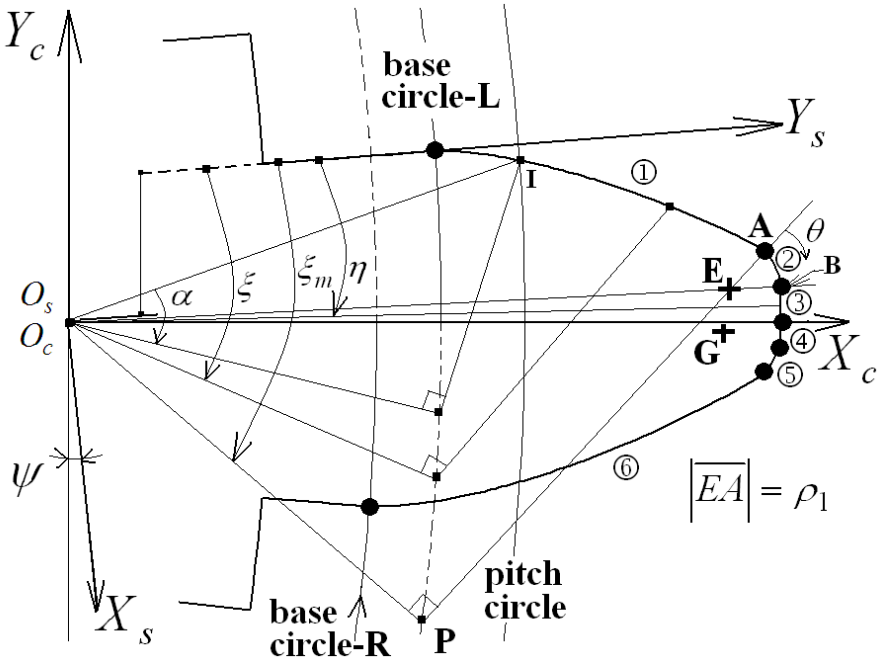

Fig. 3. Geometry of the shaper cutter

where $\psi = \pi / 2N_s + \tan\alpha - \alpha$, N_s is the number of shaper cutter teeth and α is the pressure angle of the cutter at the pitch point, as depicted in Fig. 1. Supercript i represents regions 1, 2, 3, 4, 5 and 6.

For simplicity the mathematical models of the left side generating surfaces of the cutter are given. As shown in Fig. 3., the regions 1 and 6 of the shaper cutter are used are used to generate the different sides of the working tooth surfaces of involute spur gears. ξ is the design parameter of the cutter surface which determines the location of points on the involute region and its effective range is $0 \le \xi \le \xi_m$. The position vector of region 1 is represented in the coordinate system S_s as follows (Chang & Tsay, 1998):

$$R_s^1 = \begin{Bmatrix} x_s^1 \\ y_s^1 \end{Bmatrix} = \begin{Bmatrix} r_b \sin\xi - r_b \xi \cos\xi \\ r_b \cos\xi + r_b \xi \sin\xi \end{Bmatrix} \tag{9}$$

where r_b is the radius of base circle. Substituting Eq. (9) into Eq. (8) yields the position vector of region 1 represented in coordinate system S_c as follows (Chang & Tsay, 1998):

$$R_c^1 = \begin{Bmatrix} r_b \cos(\xi - \psi) + r_b \xi \sin(\xi - \psi) \\ -r_b \sin(\xi - \psi) + r_b \xi \cos(\xi - \psi) \end{Bmatrix} \tag{10}$$

Regions 2 and 5 of the shaper cutter generate different sides of the fillet surfaces of spur gears. As shown in Fig. 1, parameter θ of the cutter surface determines the location of points on the fillet region and its effective range is $0 \le \theta \le \pi/2 - \tan^{-1}(\xi_m - (\rho_1 / r_b))$. The tangents of the involute curve and circular arc at point A should be same and continuous. Therefore, the center E of the circular arc is located on the line $\overline{PA}$, as depicted in Fig. 3. The position vector of region 2 is represented in the coordinate system S_s as follows (Chang & Tsay, 1998):

$$R_s^2 = \begin{Bmatrix} r_b \sin\xi_m - r_b \xi_m \cos\xi_m + \rho_1 \cos\xi_m + \rho_1 \cos(\theta + \xi_m) \\ r_b \cos\xi_m + r_b \xi_m \sin\xi_m - \rho_1 \sin\xi_m + \rho_1 \sin(\theta + \xi_m) \end{Bmatrix} \tag{11}$$

where ρ_1 is the radius tip fillet surface of the generating cutter, and ξ_m is the maximum extension angle of the involute curve at point A. Similarly, the position vector of region 2 can be represented in coordinate system S_c as follows:

$$R_c^2 = \begin{Bmatrix} r_b \cos(\xi_m - \psi) + r_b \xi_m \sin(\xi_m - \psi) - \rho_1 \sin(\xi_m - \psi) + \rho_1 \sin(\theta + \xi_m - \psi) \\ -r_b \sin(\xi_m - \psi) + r_b \xi_m \cos(\xi_m - \psi) - \rho_1 \cos(\xi_m - \psi) + \rho_1 \cos(\theta + \xi_m - \psi) \end{Bmatrix} \tag{12}$$

As depicted in Fig. 3, the regions 3 and 4 are used to generate the bottomland of the machined gear. η represents a design parameter of shaper cutter and its effective range is $\xi_m + \beta - \pi/2 \le \eta \le \tan\alpha - \alpha + \pi/2N_s$. Based on the cutter geometry, equation of region 3, represented in coordinate system S_s, can be expressed as (Chang & Tsay, 1998)

$$R_s^3 = \begin{Bmatrix} x_s^3 \\ y_s^3 \end{Bmatrix} = \begin{Bmatrix} r_a \sin\eta \\ r_a \cos\eta \end{Bmatrix} \tag{13}$$

where $r_a = \sqrt{r_b^2 + (r_b \xi_m - \rho_1)^2} + \rho_1$ is the radius of the tip circle of the cutter and $\beta = \pi/2 - \tan^{-1}(\xi_m - (\rho_1 / r_b))$. Similarly, the position vector of region 3 can be represented in coordinate system S_c as follows (Chang & Tsay, 1998):

$$R_c^3 = \begin{Bmatrix} x_c \\ y_c \end{Bmatrix} = \begin{Bmatrix} r_a \sin(\eta - \psi) \\ -r_a \cos(\eta - \psi) \end{Bmatrix} \tag{14}$$

Based on the differential geometry, the unit normal vectors of the above mentioned shaper cutter surface represented in coordinate system S_c are (Litvin, 1994)

$$n_c = \frac{\frac{dR_c^i}{dl_j} \times k_c}{\left| \frac{dR_c^i}{dl_j} \times k_c \right|} \tag{15}$$

where k_c is the unit vector of the Z_c-axis. Parameter l_j represents ξ, θ and η, respectively.

By substituting Eq. (10) in Eq. (15), the unit normal vector of region 1 can be obtained as follows (Chang & Tsay, 1998) :

$$n_c^1 = \begin{Bmatrix} n_{xc}^1 \\ n_{yc}^1 \end{Bmatrix} = \begin{Bmatrix} -\sin(\xi - \psi) \\ \cos(\xi - \psi) \end{Bmatrix} \tag{16}$$

By substituting Eq. (12) in Eq. (15), the unit normal vector of region 2 can be obtained as follows (Chang & Tsay, 1998):

$$n_c^2 = \begin{Bmatrix} n_{xc}^2 \\ n_{yc}^2 \end{Bmatrix} = \begin{Bmatrix} -\sin(\theta + \xi_m - \psi) \\ -\cos(\theta + \xi_m - \psi) \end{Bmatrix} \tag{17}$$

By substituting Eq. (14) in Eq. (15), the unit normal vector of region 3 can be obtained as follows (Chang & Tsay, 1998):

$$n_c^3 = \begin{Bmatrix} n_{xc}^3 \\ n_{yc}^3 \end{Bmatrix} = \begin{Bmatrix} -\sin(\eta - \psi) \\ -\cos(\eta - \psi) \end{Bmatrix} \tag{18}$$

The equations for the right side of the cutter are similar to those of left's, provided that parameters are calculated according to corresponding pressure angle, and all equations corresponding to X_c coordinate are assigned an appropriate sign.

3. Generated gear tooth surfaces

3.1 Generating with rack-cuttter

To derive the mathematical model for the complete tooth profile of involute spur gears with asymmetric teeth, coordinate systems $S_n(X_n, Y_n, Z_n)$, $S_1(X_1, Y_1, Z_1)$ and $S_h(X_h, Y_h, Z_h)$ should be set up. The coordinate systems S_n, S_1 and S_h are attached to the rack cutter, involute gear, and gear housing, respectively as shown in Fig. 4. Z_1, Z_n and Z_h are determined by the right-hand co-ordinate system. During the generation process, the rack cutter translates a distance $S = r_{p1}\,\phi_1$ while the gear blank rotates rotates by an angle ϕ_1.

The mathematical model of the generated gear tooth surface is a combination of the meshing equation and the locus of the rack cutter surfaces according to gearing theory (Litvin, 1994). Applying the following homogeneous coordinate transformation matrix equation makes it possible to obtain the locus of the cutter represented in coordinate system S_1 as follows:

$$\mathbf{R}_1^i = [M_{1n}]\mathbf{R}_c^i \tag{19}$$

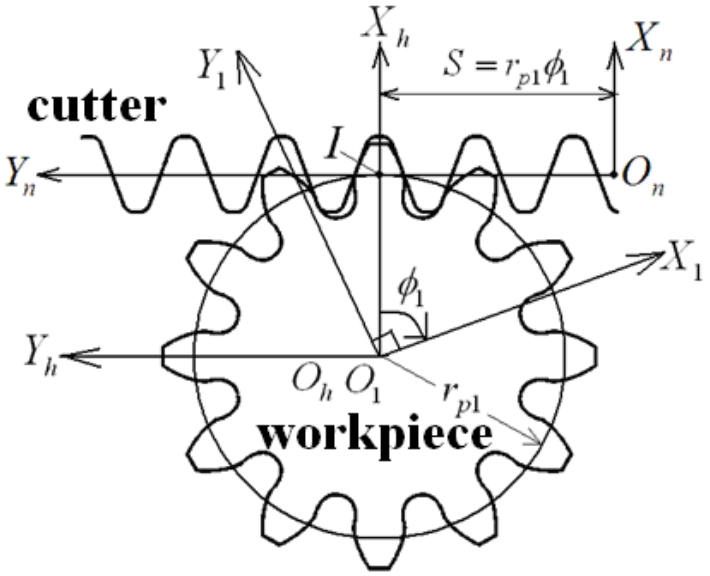

Fig. 4. Coordinate relationship between the rack cutter and the generated gear

where

$$[M_{1n}] = \begin{bmatrix} \cos\phi_1 & -\sin\phi & r_{p1}(\cos\phi_1 + \phi_1 \sin\phi_1) \\ \sin\phi_1 & \cos\phi_1 & r_{p1}(\sin\phi_1 - \phi_1 \cos\phi_1) \\ 0 & 0 & 1 \end{bmatrix}$$

According to the theory of gearing (Litvin, 1994), the common normal to the transverse section of the rack cutter and gear tooth surface must pass through the instantaneous center of rotation I. Thus, equation of meshing may be represented in coordinate system S_n as follows,

$$\frac{X_n^i - x_n^i}{n_{nx}^i} = \frac{Y_n^i - y_n^i}{n_{ny}^i} \tag{20}$$

Symbols X_c^i and Y_c^i represent the coordinates of a point on the instantaneous axis of gear rotation I-I in coordinate system S_c; x_c^i and y_c^i and are the coordinates of the instantaneous contact point on the rack cutter surface; n_{nx}^i and n_{ny}^i, are the direction cosines of the rack cutter surface unit normal $\mathbf{n}_n^i$. Angle ϕ_1 is the rolling parameter and the symbol r_{p1} denotes the radius of the gear pitch circle.

Recalling that Eq. (20) represent the equation of meshing between the generated tooth surface and the rack cutter, it can be rewritten as follows:

$$\phi_1(l_j) = (y_n^i n_{nx}^i - x_n^i n_{ny}^i)/(r_{p1} n_{nx}^i) \tag{21}$$

By simultaneously considering Eqs. (19) and (21), the mathematical model of the generated gear can now be obtained. After substitutions, the computer graph of the pinion teeth can be plotted by using an appropriate software.

3.2 Generating with pinion cutter

Figure 5 illustrates the relationship between shaper cutter and generated gear of the gear generation mechanism. The right-handed coordinate systems are considered. The coordinate system $S_f(X_f, Y_f)$ is the reference coordinate system, the coordinate system $S_g(X_g, Y_g)$ denotes the the gear blank coordinate system, and the coordinate system $S_c(X_c, Y_c)$ represents the shaper cutter coordinate system. On the basis of gear theory, the cutter rotates through an angle ϕ_c while the gear blank rotates through an angle ϕ_g. Based on the above idea, the coordinate transformation matrix from S_c to S_g can be represented as (Litvin, 1994)

$$[M_{gc}] = \begin{bmatrix} \cos(\phi_c + \phi_g) & \sin(\phi_c + \phi_g) & -(r_c + r_g)\cos\phi_g \\ -\sin(\phi_c + \phi_g) & \cos(\phi_c + \phi_g) & (r_c + r_g)\sin\phi_g \\ 0 & 0 & 1 \end{bmatrix} \tag{22}$$

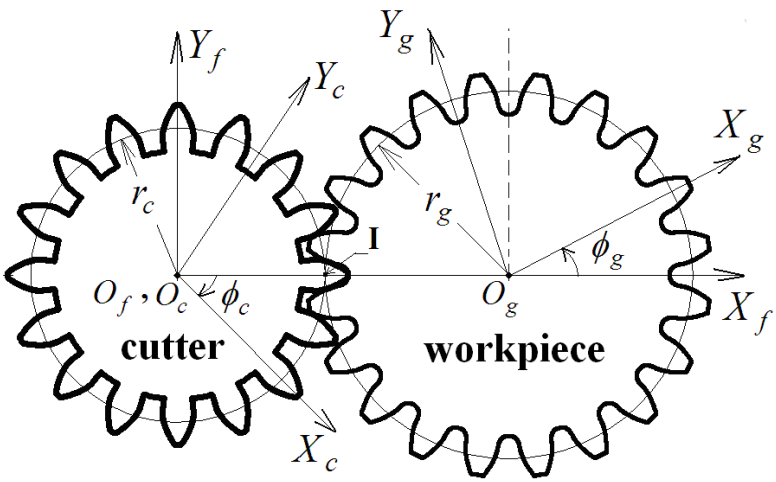

Fig. 5. Coordinate relationship between the shaper cutter and the generated gear

The relationship between the angles ϕ_g and ϕ_c is $\phi_g = (N_c / N_g)\phi_c$ where N_c is the number of teeth of the cutter and N_g denotes the number of teeth of the generated gear. Point I is

the instantaneous center of rotation and r_c and r_g are the standard pitch radii of the shaper cutter and the gear, respectively.

According to the theory of gearing (Litvin, 1994), the mathematical model of the generated gear tooth surface is a combination of the meshing equation and the locus of the rack cutter surfaces. The locus of the shaper cutter surface, expressed in coordinate system S_g, can be determined as follows (Litvin, 1994):

$$\mathbf{R}_g^i = \left[M_{gc}\right]\mathbf{R}_c^i \quad , \ (i = 1,...,6) \tag{23}$$

When two gear surfaces are meshing, both meshing surfaces should remain in tangency throughout the contact under ideal contact conditions. Conjugate tooth profiles have a common surface normal vector at the contact point which intersects the instantaneous axis of rotation (pitch point I) for a parallel axis gear pair. Therefore, the equation of meshing can be represented using coordinate system $S_c(X_c, Y_c, Z_c)$ as follows (Litvin, 1994):

$$\frac{X_c - x_c^i}{n_{cx}^i} = \frac{Y_c - y_c^i}{n_{cy}^i} \tag{24}$$

where $X_c = r_c \cos\phi_c$ and $Y_c = r_c \sin\phi_c$ are coordinates of the pitch point I represented in coordinate system S_c; x_c^i and y_c^i are the surface coordinates of the shaper cutter; symbols n_{cx}^i and n_{cy}^i symbolize the components of the common unit normal represented in coordinate system S_c. In Eqs. (23) and (24), supercript i represents regions 1 through 6 of the corresponding shaper cutter surfaces.

The mathematical model of the generated gear tooth surfaces is a combination of the meshing equation and the locus of the rack cutter surfaces according to the gearing theory. Hence, the mathematical model of the gear tooth surfaces can be obtained by simultaneously considering Eqs. (23) and (24).

4. Trochoidal paths of generating cutter

4.1 Rack cutter

In gear practice, the gometry of the tooth root fillet is of primary importance regarding the local stress concentration, which has a direct effect on the bending strength. The cutting teeth of the hobs (or rack-cutter) have generally rounded corners. During the generating process, the center of the rounding follows the trochoidal path called as primary trochoid (Su& Houser, 2000).

A general point T on the primary trochoid is depicted in Fig.6. Adopting the approach presented in (Su & Houser, 2000), following equations are derived according to the given mathematical model in a previous study of the present author (Fetvaci & Imrak, 2008). The equation of the primary trochoid which is the envelope of the center of round tip T_0 is:

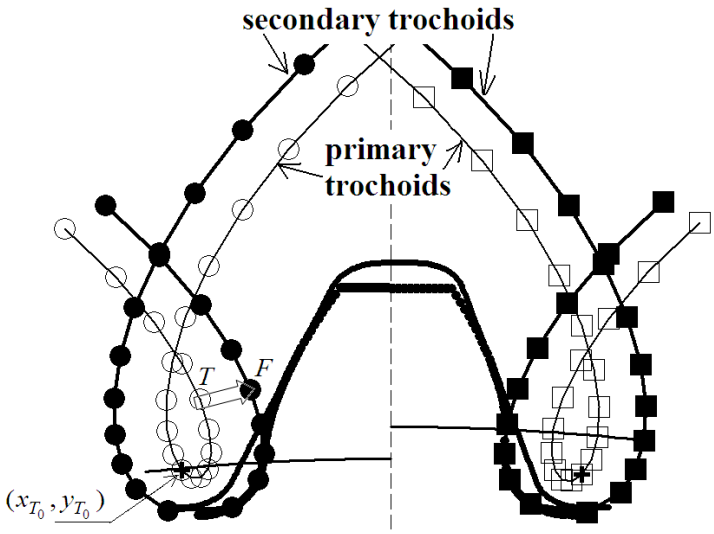

Fig. 6. Trochoidal paths of the rack-type cutter tip

$$\begin{Bmatrix} x_T \\ y_T \end{Bmatrix} = \begin{Bmatrix} x_{T_0}\cos\phi_1 - y_{T_0}\sin\phi_1 + r_{p1}(\phi_1\sin\phi_1 + \cos\phi_1) \\ x_{T_0}\sin\phi_1 + y_{T_0}\cos\phi_1 + r_{p1}(-\phi_1\cos\phi_1 + \sin\phi_1) \end{Bmatrix} \tag{25}$$

where angle ϕ_1 is the rolling parameter as stated before, r_{p1} is the radius of pitch circle (x_{T_0}, y_{T_0}) is the coordinate of point T_0 in the fixed coordinate system.

The actual form of gear tooth fillet is the envelope of the path of a series of circles equal in size to the rounding of the corner, and with their centers on the primary trochoidal path (Buckingham, 1988). This new path is called as secondary trochoid. The coordinate of the corresponding point F on the secondary trochoid can be expressed as:

$$\begin{Bmatrix} x_F \\ y_F \end{Bmatrix} = \begin{Bmatrix} x_T \\ y_T \end{Bmatrix} + \begin{Bmatrix} \rho\sin(\gamma - \phi_1) \\ \rho\cos(\gamma - \phi_1) \end{Bmatrix} \tag{26}$$

where $\gamma = \arctan(x_{T_0} / (y_{T_0} - r_{p1}\phi_1))$ and ρ denotes the tip radius of the cutter. It can be cleary seen that the primary trochoid and the secondary trochoid are two equidistant curves.

4.2 Pinion cutter

The tooth fillet resulting from gear generation is in fact a trochoid which is created by the tool tip in its rolling movement. An epitrochoid curve determines the shape of the fillet of generated external gear tooth as a result of generation process by pinion-type shaper cutters. An epitrochoid is a curve traced by a point attached to a circle of radius r rolling around the outside of a fixed circle of radius R, where the point is a distance d from the center of the exterior circle. According to the analytical mechanics of gears, the rolling circle is the pitch circle of the generating shaper cutter, the fixed circle is the pitch circle of the machined gear

and the distance d is measured from the origin of the cutter to the center of its rounded corner at the tip (point E). During the generating process of spur gear tooth presented in this paper, the center of the rounded corner at the tip traces out a trochoid. An equidistant curve with a distance of ρ defines the gear tooth root fillet.

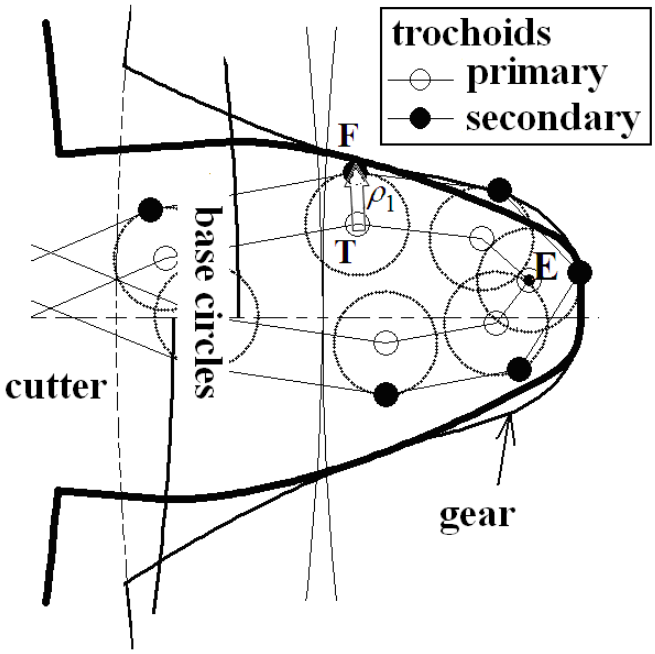

Fig. 7. Trochoidal paths of the pinion-type cutter tip

As depicted in Fig. (3) and Fig.(7), the rounded edge of the cutter is a circular arc and its center is located at point E. To ensure the tangents of the involute curve and circular arc at point A are the same and continuous, point E should be on the line $\overline{PA}$. It is first necessary to find the coordinates of points A and E (Colbourne, 1987).

The maximum involute extension angle at point A, denoted as ξ_m, can be evaluated from the following equation when the radius of tip circle r_B is given.

$$r_b \tan\xi_m = \sqrt{(r_B - \rho_1)^2 - r_b^2} + \rho_1 \tag{27}$$

According to involute geometry, the polar coordinates of point $A(r_A, \theta_A)$ are given by ,

$$r_A = r_b / \cos\xi_m \tag{28}$$

$$\theta_A = \pi / 2N_s + inv\alpha - inv\xi_m \tag{29}$$

The rectangular coordinates of point E can then be expressed in terms of x_E and y_E,

$$x_E = r_A \cos\theta_A - \rho_1 \sin(\xi_m - \theta_A) \tag{30}$$

$$y_E = r_A \sin\theta_A - \rho_1 \cos(\xi_m - \theta_A) \tag{31}$$

$$\theta_E = \tan^{-1}(y_E / x_E) \tag{32}$$

A general point on the primary trochoid which is the envelope of the center of round tip is depicted in Fig. 7. Applying the homogeneous coordinate transformation matrix given in Eq. (22), the equation of the primary trochoid (epitrochoid curve) can be written as follows:

$$\begin{Bmatrix} x_T \\ y_T \end{Bmatrix} = \begin{Bmatrix} x_E \cos(\phi_c + \phi_g) + y_E \sin(\phi_c + \phi_g) - (r_c + r_g)\cos\phi_g \\ -x_E \sin(\phi_c + \phi_g) + y_E \cos(\phi_c + \phi_g) + (r_c + r_g)\sin\phi_g \end{Bmatrix} \tag{33}$$

where (x_E, y_E) is the coordinate of point E, ϕ_c and ϕ_g are the rolling parameters, r_c and r_g are the pitch circle radius of the shaper and the machined gear, respectively.

The actual form of spur gear tooth fillet is the envelope of the path of a series of circles with their geometric centers on the primary trochoidal path. This new path is called as secondary trochoid which is the paralel curve of the primary trochoid. As a result, the coordinate of the corresponding point F on the secondary trochoid can be expressed as

$$x_F = x_T + \frac{\rho_1 y'_T}{\sqrt{x'^2_T + y'^2_T}} \tag{34}$$

$$y_F = y_T - \frac{\rho_1 x'_T}{\sqrt{x'^2_T + y'^2_T}} \tag{35}$$

where ρ_1 denotes the tip rounding radius of the shaper cutter, $x'_T = dx_T/d\phi_c$ and $y'_T = dy_T/d\phi_c$.

5. Computer graphs of tooth surfaces

Computer graphs of generating and generated surfaces can be obtained by using a programming language and graphic processor. In this study codes are developed by using GW-BASIC language to obtain the coordinates of the surfaces. GRAPHER 2-D Graphing System is used for displaying computer graphs of the cutters and gears. Also the ANSYS Preprocessor module is used for displaying gear generating process. Illustrative examples are given for both rack- and pinion-type cutters for different types of tool tip geometries.

For rack-type generation, types of tip fillet geometry are selected from the study proposed by Alipiev (Alipiev, 2009, 2011) and the related geometries displayed in the table are adopted to the present mathematical model. Table 1 displays the variation of tip geometry of the rack cutters.

		a	b
		$c_2 \rangle c_1$	$c_1 = c_2$
1	$mn \rangle \rho_1 \cos\alpha_1 + \rho_2 \cos\alpha_2$	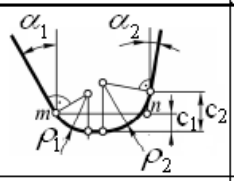	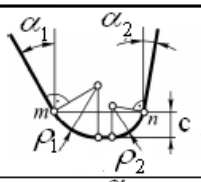
2	$mn = \rho_1 \cos\alpha_1 + \rho_2 \cos\alpha_2$	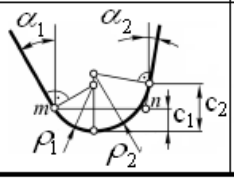	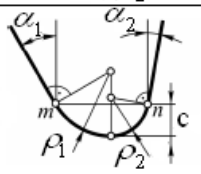

Table 1. Geometric varieties of rack tool tip (Alipiev, 2011)

As illustrated in Table 1, the rack cutter of type-1a has different clearances at its different sides. The side with a higher pressure angle has a lower radius of rounding and a lower clearance. The tooth semi-thicknesses at pitch line of the cutter are different from each other. Design parameters are selected as module $m = 2.5mm$, number of teeth $z = 24$, left side pressure angle $\alpha_1 = 20°$, right side pressure angle $\alpha_2 = 15°$, left side radius of rounding $\rho_1 = 0.2 \times m$ and right side radius of rounding $\rho_2 = 0.3 \times m$. Figure 8 displays the generating cutter of type-1a, generated surface and trochoidal paths of the tip.

As illustrated in Fig. 2. and classifed type-1b in Table 1, the cutter has a constant clearance for its all sides. The side with a higher pressure angle has a higher radius of rounding. The tooth semi-thicknesses at pitch line of the cutter are same. This type of cutter is adopted from the standard generating rack to asymmetric gearing. The relation ship between left and right side roundings is $\rho_1(1-\sin\alpha_1) = \rho_2(1-\sin\alpha_2)$. Design parameters are selected as module $m = 2.5mm$, number of teeth $z = 24$, left side pressure angle $\alpha_1 = 20°$, right side pressure angle $\alpha_2 = 15°$, left side radius of rounding $\rho_1 = 0.38 \times m$ and right side radius of rounding $\rho_2 = 0.33 \times m$. Generating and generated surfaces and trochoidal paths are illustrated in Fig 9.

Rack cutters with asymmetric teeth can also be designed with full rounded tips. The rack cutter of type-2a has a single rounded edge. The side with a higher pressure angle has a lower radius of rounding and a lower clearance. As depicted in Table 1 the centers of the rounded tip are at the center line of the cutter tooth. The tooth semi-thicknesses at pitch line of the cutter are same. Design parameters are selected as module $m = 2.5mm$, number of teeth $z = 24$, left side pressure angle $\alpha_1 = 22.5°$, right side pressure angle $\alpha_2 = 15°$, left side radius of rounding $\rho_1 = 0.4 \times m$ and right side radius of rounding $\rho_2 = 0.587 \times m$. Figure 10 displays the generating cutter of type-1a, generated surface and trochoidal paths of the tip. For visual clearity, only the corresponding halves (of secondary trochoids) that contribute to final formation of the generated tooth shape are shown.

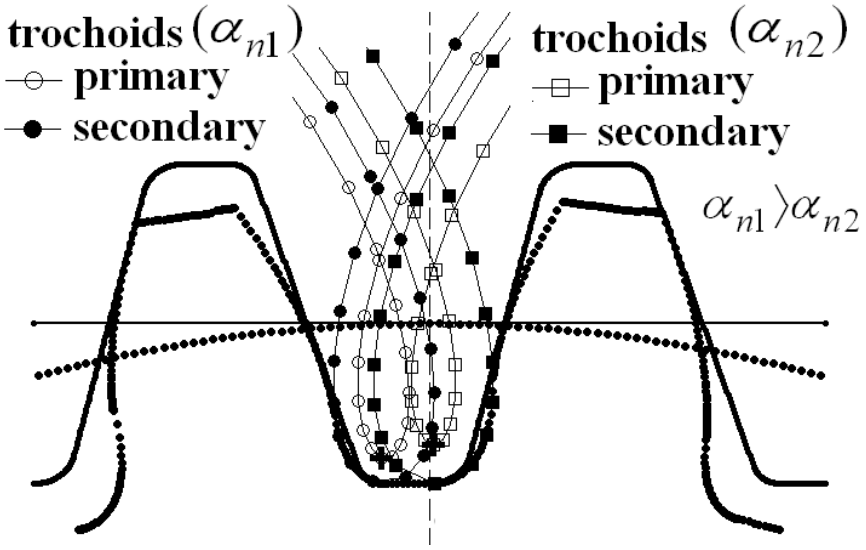

Fig. 8. Trochoidal paths of rack cutter of type-1a

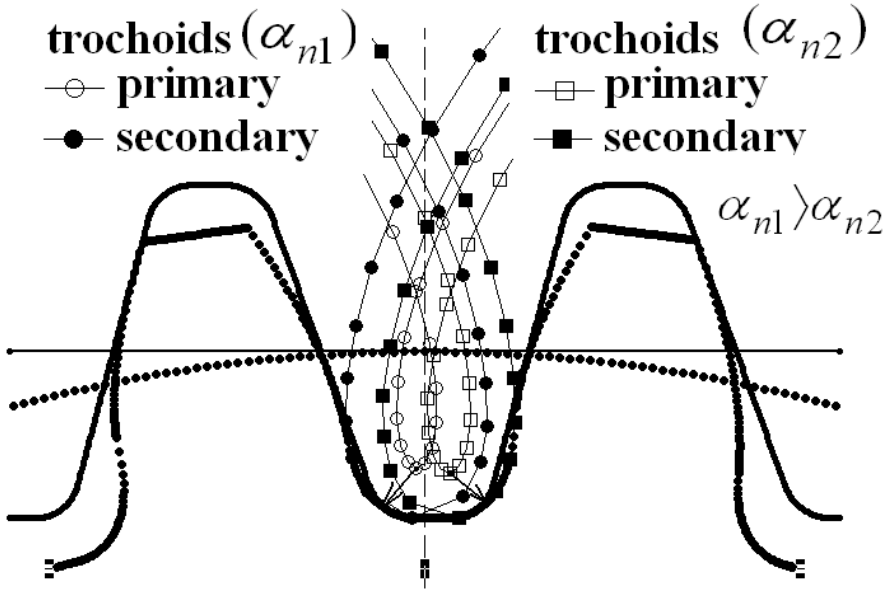

Fig. 9. Trochoidal paths of rack cutter with a rounded-tip for constant clearance

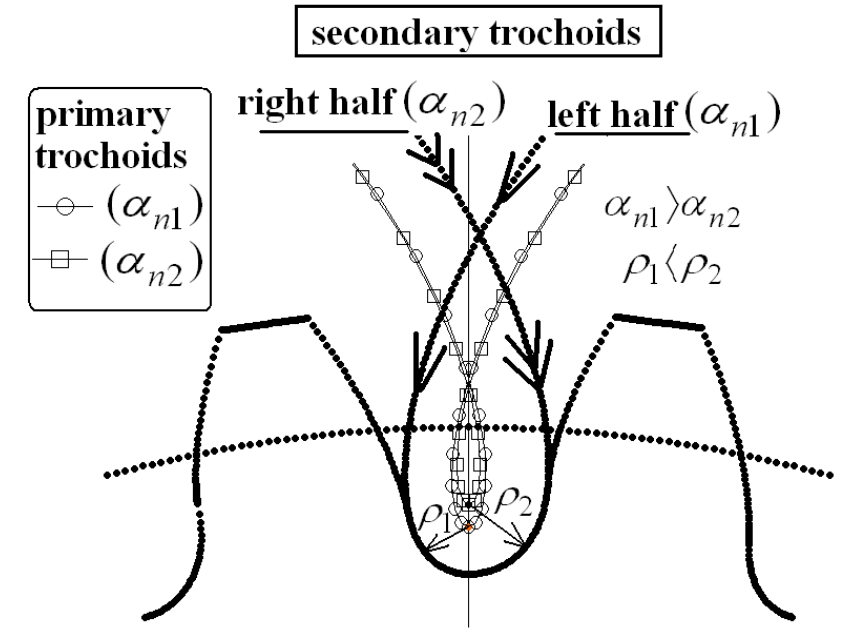

Fig. 10. Trochoidal paths of rack cutter with a fully rounded-tip

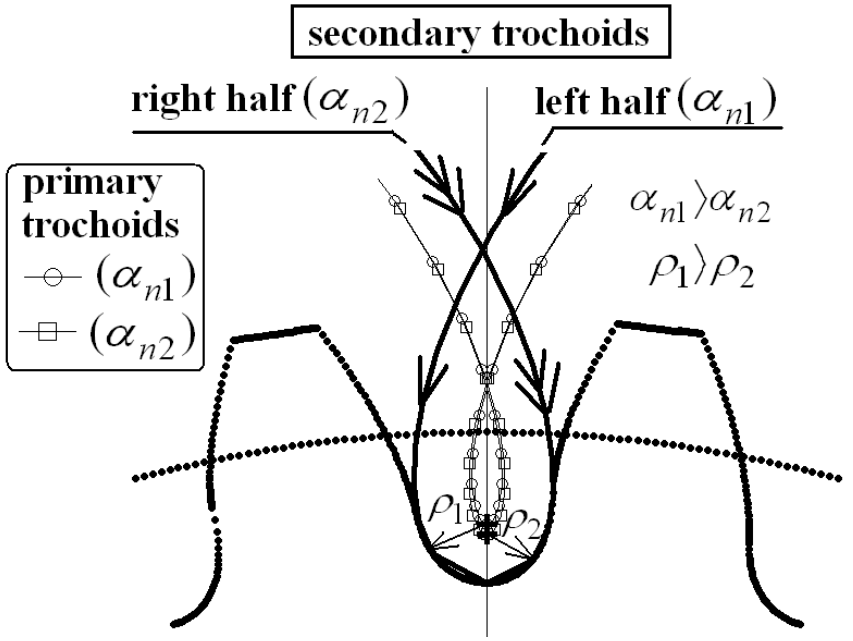

Fig. 11. Trochoidal paths of rack cutter with a fully rounded-tip for constant clearance

As classifed type-2b in Table 1, the cutter has a constant clearance for its all sides. The side with a higher pressure angle has a higher radius of rounding. The tooth semi-thicknesses at pitch line of the cutter are different. The relation ship between left and right side roundings is $\rho_1(1-\sin\alpha_1)=\rho_2(1-\sin\alpha_2)$. Design parameters are selected as module $m=2.5mm$, number of teeth $z=24$, left side pressure angle $\alpha_1=22.5°$, right side pressure angle $\alpha_2=15°$, left side radius of rounding $\rho_1=0.514\times m$ and right side radius of rounding $\rho_2=0.428\times m$. Generating and generated surfaces and trochoidal paths are illustrated in Fig. 11. For visual clearity, only the corresponding halves (of secondary trochoids) that contribute to final formation of the generated tooth shape are shown.

The geometric varieties of the rounded corner of pinion-type cutter tooth for generating symmetric and asymmetric involute gear teeth profiles can also be investigated. Illustrated examples for pinion-type generation were given by the present author (Fetvaci, 2011). Table 2 displays possible tip geometries of pinion-type shaper cutters for standard tooth height.

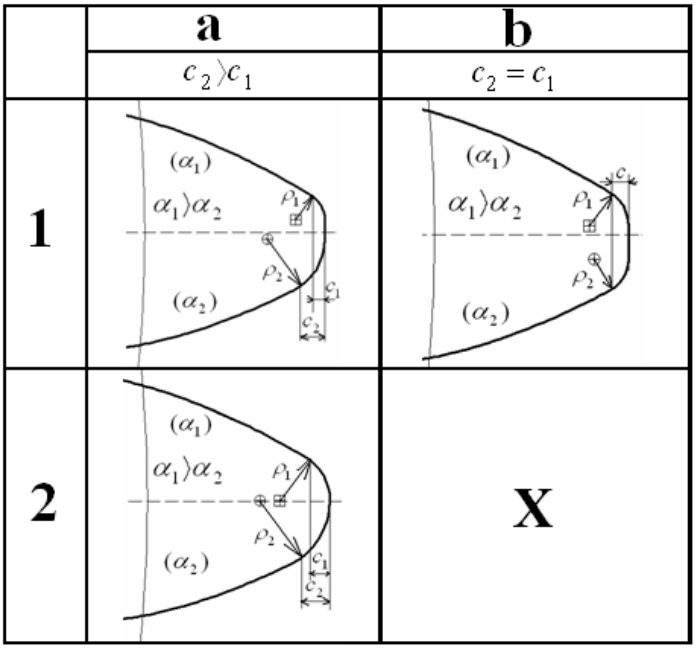

Table 2. Geometric varieties of pinion cutter tip (Fetvaci, 2011)

As illustrated in Table 2, the shaper cutter of type-1a has different clearances at its different sides. The side with a higher pressure angle has a lower radius of rounding and a lower clearance. Design parameters are selected as module $m=3mm$, number of teeth $z=20$, left side pressure angle $\alpha_1=20°$, right side pressure angle $\alpha_2=15°$, left side radius of rounding $\rho_1=0.25\times m$ and right side radius of rounding $\rho_2=0.35\times m$. Figure 12 displays the generating cutter of type-1a , generated surface and trochoidal paths of the tip.

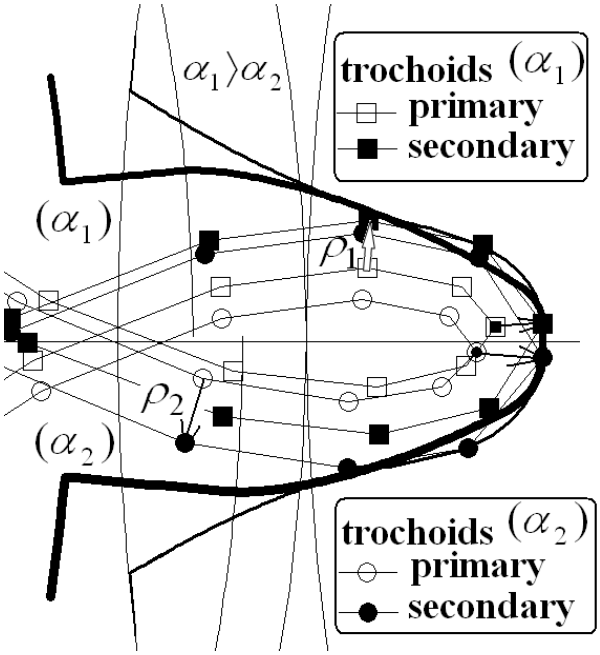

Fig. 12. Cutter with a smaller rounding radius for higher pressure angle

As illustrated in Fig. 3. and classifed type-1b in Table 2, the cutter has a constant clearance for its all sides. The side with a higher pressure angle has a higher radius of rounding. The relationship between left and right side roundings is $\rho_1(1-\sin\alpha_1)=\rho_2(1-\sin\alpha_2)$. Design parameters are selected as module $m=3mm$, number of teeth $z=20$, left side pressure angle $\alpha_1=20°$, right side pressure angle $\alpha_2=15°$, left side radius of rounding $\rho_1=0.25\times m$ and right side radius of rounding $\rho_2=0.222\times m$. Generating and generated surfaces and trochoidal paths are illustrated in Fig 13.

The shaper cutter of type-2a has a single rounded edge. The side with a higher pressure angle has a lower radius of rounding and a lower clearance. As depicted in Table 2 the centers of the rounded tip are at the center line of the cutter tooth. Design parameters are selected as module $m=3mm$, number of teeth $z=20$, left side pressure angle $\alpha_1=20°$, right side pressure angle $\alpha_2=15°$, left side radius of rounding $\rho_1=0.373\times m$ and right side radius of rounding $\rho_2=0.449\times m$. Figure 14 displays the generating cutter of type-2a , generated surface and trochoidal paths of the tip. For visual clearity, only the corresponding halves (of secondary trochoids) that contribute to final formation of the generated tooth shape are shown.

The shaper cutter with asymmetric involute teeth and with a single rounded edge can not be designed for constant clearance in case of standard tooth height. As illustrated in Fig. 3., the center of the rounding should be on the pressure line of the cutter. As a result, the geometric varieties of pinion-type tool tip is limited for indirect generation.

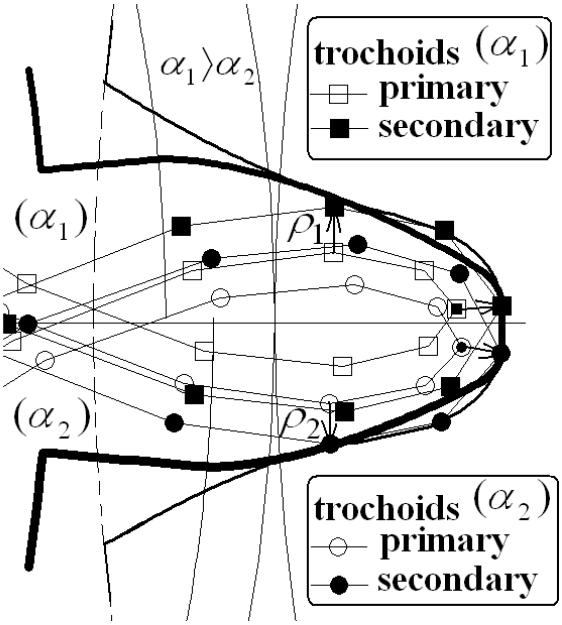

Fig. 13. Cutter with a larger rounding radius for higher pressure angle

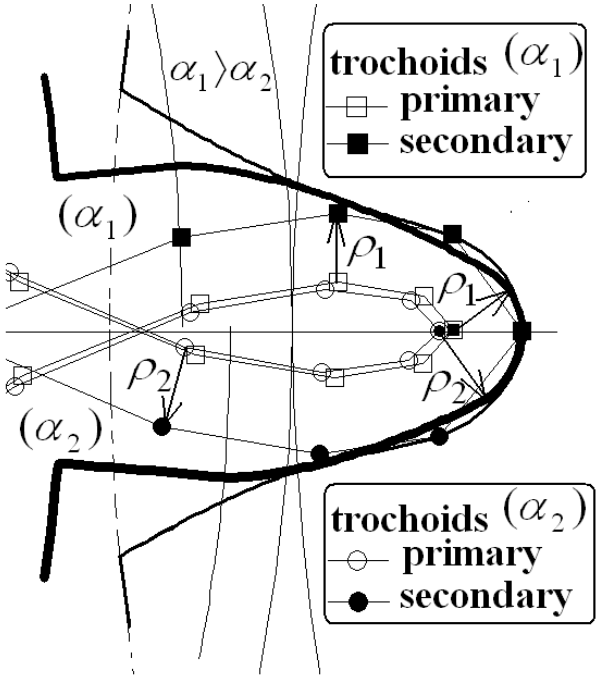

Fig. 14. Cutter with a full-rounded tip

The relative positions of the cutter during generating process can be visualized by using the mathematical of generating surfaces and transformation matrices. The present author used the locus equations of the cutters and obtained illustrations displaying simulated motion path of the cutter during generation by manipulating rolling parameter as $-\pi/4 \le \phi_1 \le \pi/4$ in the developed code. Each gear gap is produced through successive penetrations of the tool teeth into the workpiece, in the individual generating positions. This simulation can be used to determine the chip geometry (Bouzakis et al., 2008). Figure 15 displays the work gear and simulated motion path of the generating rack cutter with asymmetric teeth. Similiarly, Fig. 16. displays the work gear and simulated motion path of the generating pinion cutter.

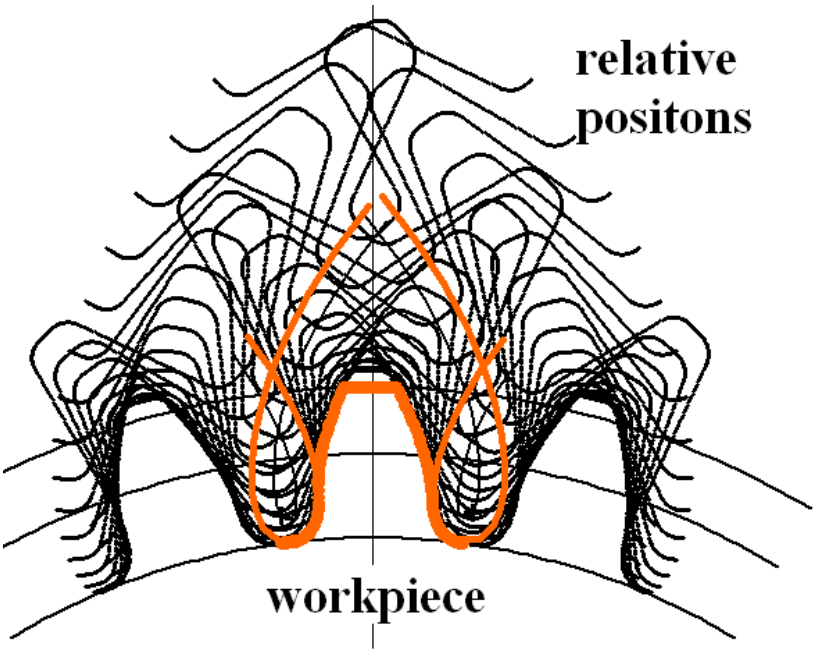

Fig. 15. Generated gear and generating positions of the rack-cutter with a rounded-tip

Figure 17 displays relative positions of the pinion cutter with symmetric involute teeth and a fully-rounded tip. The trochoidal curves exhibits symmetry according to center line of gear tooth space. Generating with a sharp-edge pinion cutter is depicted in Fig.18. In this case, primary trochoids determine the shape of the generated tooth fillet. The secondary trochoids do not exist.

Video files displaying generating positions of the cutter can be obtained with a proper software. In this study, ANSYS Parametric Design Language (APDL) is also used for obtaining graphic outputs and animation files displaying the simulated motion path of the generating cutters (ANSYS, 2009). Video files can be seen in the author's web page: http://www.istanbul.edu.tr/eng2/makina/cfetvaci/gearpage.htm

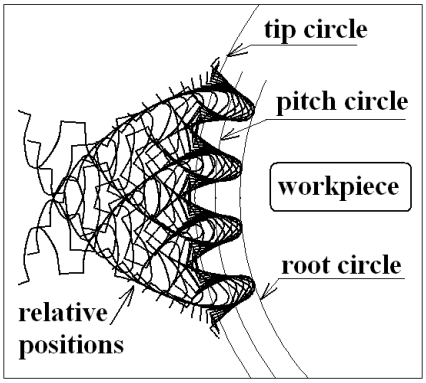

Fig. 16. Generated gear and generating positions of the pinion-cutter with a rounded-tip

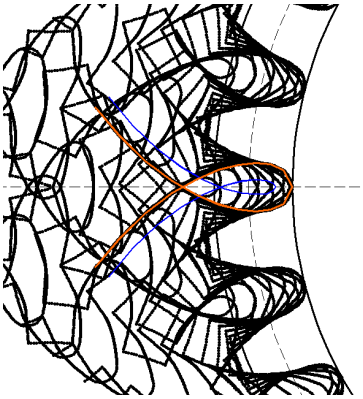

Fig. 17. Generated gear and generating positions of the pinion-cutter with symmetric teeth and a fully rounded-tip

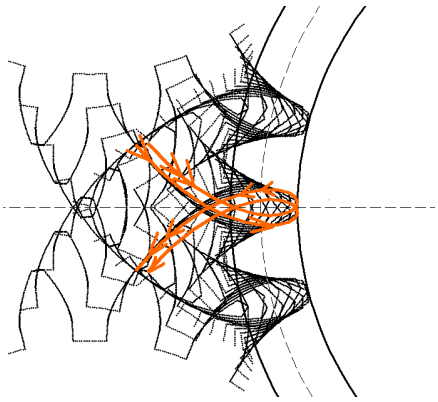

Fig. 18. Generated gear and generating positions of the pinion-cutter with symmetric teeth and a sharp-tip

6. Conclusion

In this study, computerized tooth profile generation of involute gears manufactured by rack- and pinion-type cutters are studied based on Litvin's vector method. Based on Yang's application mathematical model of rack cutter with asymmetric involute teeth is given. Trochoidal paths of the rack tool tip are investigated. For pinion-type generation Asymmetric involute teeth is adopted to Chang and Tsay's application. The developed computer program provides the investigation of the effect of tool parameters on the generated tool profile before manufactured. Trochoidal paths traced by the generating tool tip are investigated. It has been seen that geometric varieties of the rounded corner of pinion-type cutter determines the position of trochoidal paths relative to the center line of tooth space of the generated gear. Because of the position of the center of the tip rounding, there is a limitation on the geometric varieties of pinion-type cutter tip. Based on the given mathematical models, the simulated motion path of the generating cutters are also investigated. The relative position of the cutter to the workpiece has been illustrated. The simulation of shaper cutting action can be used to determine the chip geometry for further analysis about tool wear and tool life. The mathematical models can be extended to generalized mathematical model of the involute gears including spur and helical beveloid (involute conical) gears.

7. References

Alipiev, O. (2009). Geometric Synthesis of Symmetric and Asymmetric Involute Meshing using the Method of Realized Potential. *General Machine Design Conference*, p. 43-50, Ruse – Bulgaria, October 15-16, 2009

Alipiev, O. (2011). Geometric Design of Involute Spur Gear Drives with Symmetric and Asymmetric Teeth using the Realized Potential Method. *Mechanism and Machine Theory*, Vol. 46, No. 1, (January 2011), pp. 10-32, ISSN 0094-114X

ANSYS. (2009). *ANSYS Parametric Design Language Guide*. Available from, http://www1.ansys.com/customer/content/documentation/120/ans_apdl.pdf

Bouzakis, K.-D., Lili, E., Michailidis, N. & Friderik, O. 2008. Manufacturing of Cylindrical Gears by Generating Cutting Processes: A Critical Synthesis of Analysis Methods. *CIRP Annals - Manufacturing Technology*, Vol. 57, No.2, 2008, pp. 676-696.

Buckingham, E. (1949). *Analytical Mechanics of Gears*, McGraw-Hill, New York, USA

Chang, S.-L. & Tsay, C.-B. (1998). Computerized Tooth Profile Generation and Undercut Analysis of Noncircular Gears Manufactured with Shaper Cutters. *Journal of Mechanical Design*, Vol. 120, No. 1, (March 1998), pp. 92-99.

Chen, C.-F & Tsay, C.-B. (2005). Tooth Profile Design for the Manufacture of Helical Gear Sets with Small Numbers of Teeth, *International Journal of Machine Tools and Manufacture*, Vol. 45, No. 12-13, (October 2005), pp. 1531-1541

Colbourne, J.R. (1987). *The Geometry of Involute Gears*, Springer-Verlag, New Jersey, USA

Fetvaci, C. & İmrak, E. (2008). Mathematical Model of a Spur Gear with Asymmetric Involute Teeth and its Cutting Simulation. *Mechanics Based Design of Structures and Machines* , Vol. 36, No. 1, pp. 34- 46, ISSN 1539-7734

Fetvacı, C. (2010a). Definition of Involute Spur Gear Profiles Generated By Gear-Type Shaper Cutters. *Mechanics Based Design of Structures and Machines*. Vol.38, No. 4, pp. 481-492

Fetvaci, C. (2010b). Computer Simulation of Helical Gears with Asymmetric Involute Teeth. *Journal of The Faculty of Engineering and Architecture of Gazi University*, Vol. 25, No. 3, (September 2010), pp. 441-447, ISSN 1300-1884

Fetvaci, C. (2011). Computer Simulation of Asymmetric Involute Spur Gears Manufactured by Generating-Type Cutters . *Engineers and Machinery*, Vol. 52, No. 616, (May 2011), pp. 60-69

Figliolini, G. & Angeles, J. (2003). The Synthesis of Elliptical Gears Generated by Shaper-Cutters. *Journal of Mechanical Design*, Vol.125, No. 4, (December 2003), pp. 793-801, 2003.

Lin, T., Ou, H. & Li, R. (2007). A Finite Element Method for 3-D Static and Dynamic Contact/Impact Analysis of Gear Drives. *Computer Methods in Applied Mechanics and Engineering*. Vol. 196, No. 9-12, (February 2007), pp. 1716-1728.

Litvin, F.L. (1994). *Gear Geometry and Applied Theory*, Prentice Hall, New Jersey, USA

Muni, D.V., Kumar, S. & Muthuveerappan, G. (2007). Optimization of Asymmetric Spur Gear Drives for Maximum Bending Strength Using Direct Gear Design Method. *Mechanics Based Design of Structures and Machines*, Vol.35, No.2, pp. 127-145

Salamoun, C. & Suchy, M. (1973). Computation of Helical or Spur Gear Fillets. *Mechanism and Machine Theory*, Vol. 8, No. 3, (Autumn 1973), pp. 305-322, ISSN 0094-114X

Su, X. & Houser, D.R. (2000). Characteristics of Trochoids and their Application to Determining Gear Teeth Fillet Shapes. *Mechanism and Machine Theory*, Vol. 35, No. 2, (February 2000), pp. 291–304, ISSN 0094-114X

Tang, X., Ren, F., Jiang, Y. & Gao, S. (2008). Geometric Modeling and Dynamic Simulation of Involute Gear by Generating Method, *Proceedings 13th International Conference on Geometry and Graphics*, pp. 233-234, Dresden, Germany, August 4-8, 2008

Tsay, C.-B. (1988). Helical Gears with Involute Shaped Teeth: Geometry, Computer Simulation, Tooth Contact Analysis and Stress Analysis. *Journal of Mechanical Design*, Vol. 110, No. 4 , pp. 482-491

Yang, S.-C. (2005). Yang, Mathematical Model of a Helical Gear with Asymmetric Involute Teeth and its Analysis. *International Journal of Advanced Manufacturing Technology*, Vol. 26, No. 5-6, (September 2005), pp. 448-456, ISSN 0268-3768

Yang, S.-C. (2007). Study on an Internal Gear with Asymmetric Involute Teeth. *Mechanism and Machine Theory*, Vol. 42, No. 8, (August 2007), pp. 977-994

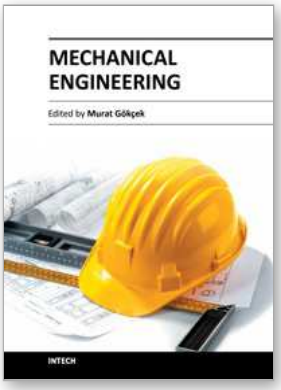

Mechanical Engineering

Edited by Dr. Murat Gokcek

ISBN 978-953-51-0505-3
Hard cover, 670 pages
Publisher InTech
Published online 11, April, 2012
Published in print edition April, 2012

The book substantially offers the latest progresses about the important topics of the "Mechanical Engineering" to readers. It includes twenty-eight excellent studies prepared using state-of-art methodologies by professional researchers from different countries. The sections in the book comprise of the following titles: power transmission system, manufacturing processes and system analysis, thermo-fluid systems, simulations and computer applications, and new approaches in mechanical engineering education and organization systems.

How to reference

In order to correctly reference this scholarly work, feel free to copy and paste the following:

Cuneyt Fetvaci (2012). Computer Simulation of Involute Tooth Generation, Mechanical Engineering, Dr. Murat Gokcek (Ed.), ISBN: 978-953-51-0505-3, InTech, Available from: http://www.intechopen.com/books/mechanical-engineering/computer-simulation-of-involute-tooth-generation

INTECH
open science | open minds

InTech Europe
University Campus STeP Ri
Slavka Krautzeka 83/A
51000 Rijeka, Croatia
Phone: +385 (51) 770 447
Fax: +385 (51) 686 166
www.intechopen.com

InTech China
Unit 405, Office Block, Hotel Equatorial Shanghai
No.65, Yan An Road (West), Shanghai, 200040, China
中国上海市延安西路65号上海国际贵都大饭店办公楼405单元
Phone: +86-21-62489820
Fax: +86-21-62489821